Polarization of Macrophages, Cellular Adhesion, and Spreading on Bacterially Contaminated Gold Nanoparticle-Coatings in Vitro

Luan, Yafei; van der Mei, Henny C.; Dijk, Melissa; Geertsema-Doornbusch, Gesinda; Atema-Smit, Jelly; Ren, Yijin; Chen, Hong; Busscher, Henk J.

Published in:
ACS Biomaterials Science & Engineering

DOI:
10.1021/acsbiomaterials.9b01518

Publication date:
2020

ACS Biomaterials SCIENCE & ENGINEERING

pubs.acs.org/journal/abseba

Article

Polarization of Macrophages, Cellular Adhesion, and Spreading on Bacterially Contaminated Gold Nanoparticle-Coatings *in Vitro*

Yafei Luan, Henny C. van der Mei,* Melissa Dijk, Gésinda I. Geertsema-Doornbusch, Jelly Atema-Smit, Yijin Ren, Hong Chen,* and Henk J. Busscher

Cite This: *ACS Biomater. Sci. Eng.* 2020, 6, 933–945

Read Online

ACCESS | Metrics & More | Article Recommendations | Supporting Information

ABSTRACT: Biomaterial-associated infections often arise from contaminating bacteria adhering to an implant surface that are introduced during surgical implantation and not effectively eradicated by antibiotic treatment. Whether or not infection develops from contaminating bacteria depends on an interplay between bacteria contaminating the biomaterial surface and tissue cells trying to integrate the surface with the aid of immune cells. The biomaterial surface plays a crucial role in defining the outcome of this race for the surface. Tissue integration is considered the best protection of a biomaterial implant against infectious bacteria. This paper aims to determine whether and how macrophages aid osteoblasts and human mesenchymal stem cells to adhere and spread over gold nanoparticle (GNP)-coatings with different hydrophilicity and roughness in the absence or presence of contaminating, adhering bacteria. All GNP-coatings had identical chemical surface composition, and water contact angles decreased with increasing roughness. Upon increasing the roughness of the GNP-coatings, the presence of contaminating *Staphylococcus epidermidis* in biculture with cells gradually decreased surface coverage by adhering and spreading cells, as in the absence of staphylococci. More virulent *Staphylococcus aureus* fully impeded cellular adhesion and spreading on smooth gold- or GNP-coatings, while *Escherichia coli* allowed minor cellular interaction. Murine macrophages in monoculture tended toward their pro-inflammatory "fighting" M1-phenotype on all coatings to combat the biomaterial, but in bicultures with contaminating, adhering bacteria, macrophages demonstrated Ym1 expression, indicative of polarization toward their anti-inflammatory "fix-and-repair" M2-phenotype. Damage repair of cells by macrophages improved cellular interactions on intermediately hydrophilic/rough (water contact angle 30 deg/surface roughness 118 nm) GNP-coatings in the presence of contaminating, adhering Gram-positive staphylococci but provided little aid in the presence of Gram-negative *E. coli*. Thus, the merits on GNP-coatings to influence the race for the surface and prevent biomaterial-associated infection critically depend on their hydrophilicity/roughness and the bacterial strain involved in contaminating the biomaterial surface.

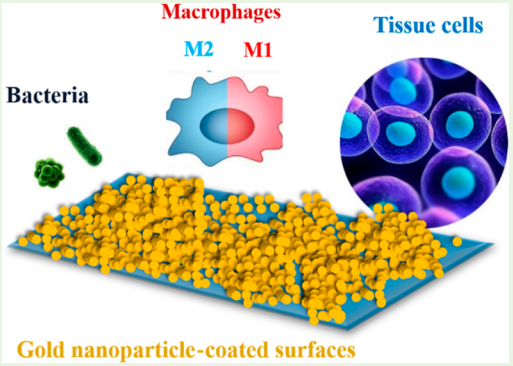

KEYWORDS: *triculture, race for the surface, nanostructured surface, Ym1, cytokines, IL-10, biomaterial-associated infection*

INTRODUCTION

Long life expectancy and the preservation of a high quality of life necessitate the use of biomaterials implants and devices once disease, oncological surgery, injury, or wear have caused irreparable damage to the human body. Biomaterials implants and devices fail at an unacceptable rate of around 5% across different applications.[1−3] One of the main reasons is bacterial colonization of the biomaterial surface, with bacteria spreading off into adjacent tissues.[4] Bacteria can contaminate the biomaterial surface or surgical site in low-level adhering numbers during implantation or hospitalization, to cause acute, usually severe[5] or lingering, low-grade infections.[6] Bacteria introduced during implantation or hospitalization can remain dormant for several years, during which they are insensitive to antibiotics, before they can cause clear clinical signs of infection or cause acute infection within days after implantation.[2,7] Acute infection due to highly virulent pathogens like *Staphylococcus aureus* or *Escherichia coli* is accompanied by severe pain, high fever, and obvious indications of infection such as elevated levels of C-reactive protein, erythrocyte sedimentation, and white blood cell count.[5,8] The aggressiveness of a biomaterial-associated infection painfully follows from a case report on a patient who died 4 days after pacemaker replacement, while symptoms were being mistaken for the flu.[5] On the other hand, low-grade infections associated with biomaterials implants and devices can be caused by commensals of the skin, such as *Staphylococcus epidermidis*[6] that can linger longtime. An

Received: October 4, 2019
Accepted: January 14, 2020
Published: January 15, 2020

https://dx.doi.org/10.1021/acsbiomaterials.9b01518
ACS Biomater. Sci. Eng. 2020, 6, 933–945

example is the case study on a 14 year old boy colliding with a truck and acquiring an open fracture of the right leg.[5] After placing an external fixator, the wound swelled after 10 days, the fixator pins were removed, a cannulated tibia nail was placed, and the boy was hospitalized for another 10 days. After another 3 weeks the boy had fever, leg pain, swelling, and a draining fistula in his leg. Multiple antibiotic treatments followed over the course of 2 years, resulting eventually in extensive osteomyelitis treatment and replacement of the tibia nail. With the increasing number of antibiotic-resistant bacterial strains and species posing an ever-growing threat, new antimicrobial strategies have to be developed to prevent the development of biomaterial-associated infections, in which nanotechnology will play an important role.[9,10] Nanostructured surfaces preventing the development of biomaterial implant- and device-associated infections after per-operative bacterial contamination would greatly reduce their failure rate.

Nanopillared surfaces, for example, can induce production of extracellular polymeric substances upon adhesion due to high localized pressures on the bacterial cell wall that can ultimately lead to bacterial cell death.[11−14] Gold nanoparticle (GNP)-coatings have been demonstrated to reduce *S. epidermidis* biofilm thickness and viability as compared with smooth gold surfaces[12] and amplified the function of RGD peptides to stimulate adhesion of tissue cells.[15] Although it is known that immune cells are frustrated in the general performance of their tasks in the presence of biomaterial implants and devices, little is known about their behavior on nanostructured surfaces. Nanostructured, 30 nm rough TiO_2 surfaces kept macrophages in their pro-inflammatory,[16] M1-phenotype that can cause damage to tissue cells through production of reactive oxygen species[17] but at the same time fights bacterial infections.[18] However, 80 nm rough TiO_2 surfaces stimulated polarization to the anti-inflammatory,[16] "fix-and-repair" M2-phenotype,[17,19,20] facilitating tissue repair and production of extracellular matrix.

Most evaluations of infection-resistant biomaterial surfaces, including the above examples, are based on monoculture studies that comprise a biomaterial combined with either tissue cells, immune cells, or bacteria.[16] *In vivo* however, the true fate of a biomaterials implant or device depends on an interplay between tissue integration, bacterial colonization, immune cell activity, and the properties of the biomaterial surface. Tissue integration prevailing over bacterial colonization is generally accepted to provide the best long-term protection of biomaterial implants and devices against infection.[21,22] Obviously, this interplay, named "the race for the surface" by the late orthopedic surgeon Gristina, cannot be studied in monoculture experiments with only bacteria or cells.[22,23] Driven by growing doubts on the relevance of animal studies with respect to predicting human clinical study outcomes,[24,25] we have developed coculture models, comprising tissue cells, bacteria, and macrophages to evaluate the outcome of the race for the surface.[26] Biculture studies with different bacterial strains and tissue cells have demonstrated that *S. aureus* is much more aggressive toward tissue cells in their race for the surface than *S. epidermidis*.[27−29] Human gingival tissue cells were more effective in their race for dental implant surfaces with contaminating oral bacteria on smooth titanium surfaces than on other materials,[30] which is in line with large scale, human clinical trials.[31] Corresponding with clinical findings, tricultures demonstrated that macrophages were effective in aiding tissue cells to win the race for the surface, depending on bacterial virulence.[32,33] Accordingly, coculture studies have been advocated as a possible bridge to human clinical studies, with the possibility to strongly reduce, if not eliminate, the need for animal experiments.[26]

This paper aims to determine whether GNP-coatings with a specific hydrophilicity and roughness can be identified that present maximal opportunities for osteoblasts and human mesenchymal stem cells to win the race for these surfaces, when contaminated with a low number of adhering bacteria with or without the aid of macrophages. In addition, it will be determined whether macrophages tend toward polarization in their pro-inflammatory M1- or anti-inflammatory M2-phenotype on different bacterially contaminated GNP-coatings. To this end, different mono- and cocultures will be set up involving three bacterial strains (*S. aureus*, *E. coli*, or *S. epidermidis*), common in biomaterial implant and device associated infections.

EXPERIMENTAL SECTION

Materials. Hydrogen tetrachloroaurate hydrate acid ($HAuCl_4 \cdot 4H_2O$) and glucose were purchased from Sinopharm Chemical Reagent Co. (Shanghai, China). Potassium hydrogen carbonate (AR) was purchased from Shanghai Zhanyun Chemical Co. (Shanghai, China). Tryptone soy broth (TSB) and brain heart infusion (BHI) were purchased from Oxoid (Basingstoke, UK). Dulbecco's modified Eagle's medium supplemented with 1 g/L D-glucose (DMEM-LG), Dulbecco's modified Eagle's medium supplemented with high glucose (DMEM-HG), α-modified Eagle's medium (α-MEM), and fetal bovine serum (FBS) were all purchased from Invitrogen (Breda, The Netherlands). β-Cysteamine (C_2H_7NS, 95%), ascorbic acid-2-phosphate (AA2P), Triton X-100, phalloidin-FITC, and 6-diamidino-2-phenylindole (DAPI) were purchased from Sigma-Aldrich Chemie B.V. (Zwijndrecht, The Netherlands). Acetone, ethanol (100%), and all other solvents were purchased from Merck KGaA (Darmstadt, Germany) and used as received. All aqueous solutions were prepared in ultrapure water (Sartorius arium 611DI ultrapure water system) to give a minimum resistivity of 18.2 MΩ·cm (Sartorius, Göttingen, Germany).

Preparation and Characterization of Gold Nanoparticle-Coated Surfaces. Gold nanoparticle (GNP)-coated surfaces were fabricated, as described previously.[34,35] Briefly, polished silicon wafers were coated with a 10 nm thick chromium layer to support an 80 nm thick gold coating. Next, wafers were cut into 0.5 × 0.5 cm^2 samples, rinsed with acetone, treated for 30 min with ozone plasma, washed with freshly prepared Piranha solution (H_2SO_4/H_2O_2, 7:3 v/v) at room temperature, and extensively washed with demineralized water. Subsequently, the cleaned gold-coated wafers were dried under nitrogen, immersed in a 20 mM β-cysteamine ethanol solution overnight at room temperature, rinsed with ethanol, dried with nitrogen, and placed in a 48-well plate. After adjusting the temperature to 37 °C and the pH of the solution to pH 9, different volumes of GNP-suspensions were added. After 8 h of sedimentation, suspensions were removed from the wells, and wafers were washed with demineralized water and finally dried in air to obtain GNP-coated surfaces with a different density of GNPs on the wafer surface and therewith different surface roughnesses.

Roughness of the gold- and GNP-coated surfaces was measured by Atomic Force Microscopy (AFM; Multi-Mode Nanoscope V, Bruker, Santa Barbara, CA) with an NP-10 nonconductive silicon nitride tip (Bruker, nominal spring constant 0.58 N/m, resonance frequency 40−75 kHz) in the tapping mode. The evaluation area for each sample was 20 × 20 μm^2. Surface roughness was expressed as an arithmetic mean (R_a), as obtained directly from the NanoScope Analysis software (Bruker). In addition, surface morphology of coated surfaces was visualized using scanning electron microscopy (SEM, S-4700, Hitachi) at 15.0 kV. Equilibrium water contact angles were measured on all samples using the sessile drop method on an SL200C

https://dx.doi.org/10.1021/acsbiomaterials.9b01518
ACS Biomater. Sci. Eng. 2020, 6, 933−945

optical contact angle meter (Solon Information Technology Co., Ltd. Georgia, USA) at room temperature.

The chemical composition of the gold-coated surfaces was determined using X-ray Photoelectron Spectroscopy (XPS, S-probe, Surface Science Instruments, Mountain View, CA, USA), operated at a vacuum of 10^{-9} Pa. The X-ray (10 kV, 22 mA) beam was produced using an aluminum anode and had a spot size of 250 × 1,000 μm. Wide-scan spectra in the binding energy range of 1−1300 eV and narrow scans of 50 eV were made of carbon (282−290 eV), oxygen (530−536 eV), gold (82−92 eV), and nitrogen (396−403 eV) from which the elemental composition of the surfaces was calculated.

Bacteria, Culture Conditions, and Harvesting. Two Gram-positive staphylococcal strains, *S. aureus* ATCC 12600 and *S. epidermidis* ATCC 12228, and a Gram-negative *E. coli* strain (ATCC 25922) were used in this study (all obtained from the American Type Culture Collection). The strains were grown on blood agar plates from frozen stock and incubated aerobically at 37 °C overnight. Agar plates were subsequently stored in the refrigerator at 4 °C. One colony was inoculated in 10 mL of TSB for staphylococci or BHI for *E. coli* ATCC 25922 and incubated at 37 °C for 24 h. This preculture was added to 200 mL of TSB or BHI, which was grown for 16 h at 37 °C before harvesting. Bacteria were harvested by centrifugation at 5000*g* for 5 min at 10 °C followed by washing twice with sterile phosphate buffered saline (PBS, 10 mM potassium phosphate, 0.15 M NaCl, pH 7.0). The bacterial suspension was sonicated 10 s for 3 times to separate bacterial aggregates. The bacterial concentration in PBS was determined using a Bürker-Türk counting chamber and adjusted to meet the requirements of the different experiments.

Viability of Bacteria Adhering on Gold- and GNP-Coated Surfaces. Gold- and GNP-coated surfaces were sterilized with 70% ethanol and washed with sterile demineralized water 3 times for 5 min each and placed in a 48-well plate. One milliliter of bacterial suspension (3×10^6 bacteria per mL in PBS) was added to the wells with the gold- and GNP-coated samples and left to sediment for 3 h at room temperature to create equal numbers of adhering bacteria on each surface (around 1.7×10^5 cm^{-2}). After 3 h, the sample surfaces were rinsed with sterile PBS and stained with a live/dead staining solution, containing 3.34 mM SYTO 9 and 20 mM propidium iodide (*Bac*Light, Molecular Probes Inc., Waltham, MA USA) for 15 min in the dark, also at room temperature. After gently rinsing with PBS, adhering live and dead bacteria were observed by fluorescence microscopy (DM 4000B, Leica, Wetzlar, Germany) with a 40× objective, and images of 5 randomly chosen fields of view were taken from each sample. The number of bacteria in each image was analyzed with the Image-Pro Plus software to obtain the average number of adhering live and dead bacteria, which were subsequently expressed as a percentage of dead bacteria with respect to the total number of bacteria on a surface. Each experiment was repeated three times with newly prepared samples and separately cultured bacteria.

Biofilm Formation on Gold- and GNP-Coated Surfaces. The sterile gold- and GNP-coated surfaces were placed in a 48-well plate, and 1 mL of bacterial suspension of 3×10^8 bacteria per mL in PBS was added and left at room temperature for 3 h to allow initial bacterial adhesion. Next, the bacterial suspension was removed, and 1 mL of TSB (staphylococci) or BHI (*E. coli* ATCC 25922) was added to each well and incubated at 37 °C for 48 h to allow growth of the adhering bacteria into a biofilm. The culture medium was refreshed after 24 h. After 48 h, the sample surfaces with adhering biofilms were rinsed gently 3 times with sterile PBS and biofilm thickness measured by optical coherence tomography (OCT, Ganymade, Thorlabs Inc., Munich, Germany) in PBS. A spectral domain of the OCT with an axial resolution of 5.8 μm and a lateral resolution of 8 μm were used to obtain images. OCT allows *in situ* imaging of biofilms without additional staining over a large sample area. Each experiment was repeated three times with newly prepared samples and separately cultured bacteria.

Cell Lines, Culture Conditions, and Harvesting. Human osteosarcoma (U2OS, ATCC HTB-96 obtained from LGC, Wesel, Germany), human mesenchymal stem cells (hMS, MSC PT-2501 obtained from a 40 year old female, Lonza, Basel, Switzerland), and murine macrophages J774A.1 (ATCC TIB-67, also obtained from LGC) were used in this study. U2OS cells were grown in tissue-culture polystyrene flasks (Greiner Bio-One GmbH, Frickenhausen, Germany) in DMEM-LG, 10% FBS, and 0.2 mM AA2P, hMS cells were grown in α-MEM, 10% FBS, and 0.2 mM AA2P, and macrophages were grown in DMEM-HG, 10% FBS, and 0.2 mM AA2P at 37 °C in a humidified 5% CO_2 incubator. U2OS and hMS cells were harvested at 80−90% confluency by trypsin-EDTA treatment and centrifugation at 1200 rpm, while macrophages were harvested manually using a cell scraper at 80−90% confluency. After harvesting, cells were suspended in DMEM-HG, and their concentrations were adjusted to 1.5×10^4 per mL using a Scepter cell counter (Millipore, Amsterdam, The Netherlands).

Cytotoxicity of the GNP-Coated Surfaces. Cytotoxicity of the GNP-coatings was established toward U2OS, hMS cells, and J774A.1 macrophages, using the CCK-8 assay based on metabolic activity of the cells.[36] U2OS, hMS, and J774A.1 macrophages (1.5×10^4 per mL, 2 mL) were seeded in a 24-well plate with or without a gold- or GNP-coated sample for 24 h at 37 °C in a humidified 5% CO_2 incubator. Then, the cell culture medium was replaced by 400 μL of the appropriate cell culture medium with 40 μL of CCK-8 solution in each well. After incubation at 37 °C for 2 h, the absorbance was measured at 450 nm using a microplate reader (Thermo Fisher Scientific, Waltham, USA) and expressed as relative viability, equating the absorbance after growth on tissue-culture polystyrene, to 100%.

Cell Adhesion and Spreading on Gold- and GNP-Coated Surfaces. Next, adhesion and spreading of U2OS and hMS cells were determined on gold- and GNP-coated surfaces. To this end, a 2 mL cell suspension was seeded in a 24-well plate together with a gold- or GNP-coated surface. After incubation at 37 °C in a humidified 5% CO_2 incubator for 24 h, the samples were rinsed with PBS and fixed with 3.7% paraformaldehyde in cytoskeleton stabilization buffer (0.1 M Pipes, 1 mM EGTA, 4% (w/v) polyethylene glycol 8000, pH 7.0) for 10 min. Fixed cells were permeabilized with 0.5% Triton X-100 in PBS for 3 min and stained with 2 μg/mL phalloidin-FITC and 4 μg/mL DAPI in PBS with 1% bovine serum albumin (BSA) for 30 min. The number of adhering cells and their surface coverage were determined using fluorescent microscopy, and the number of cells and their spreading were analyzed with Scion image analysis software. Five images of each sample surface were taken randomly for enumeration. All experiments were performed in triplicate for each cell line with separately grown cells.

Bicultures of Tissue Cells and Bacteria on Gold- and GNP-Coated Surfaces. Biculture experiments were performed with staphylococci and *E. coli* in coculture with U2OS and hMS cells. To obtain a level of bacterial contamination per unit area of 250/cm^2 equal as found in per-operative contamination,[37] smooth gold- and GNP-coated surfaces placed in a 48-well plate were immersed in 1 mL bacterial suspensions (1×10^3 bacteria per mL) for 1 h at room temperature. The wafers were rinsed 3 times with sterile PBS, followed with seeding of cells from 2 mL of suspension (1.5×10^4 per mL) in modified growth medium allowing both cellular growth and growth of all three bacterial strains. Modified growth medium was developed according to a previously published protocol,[21] yielding DMEM-LG supplemented with 2% TSB for U2OS or α-MEM for hMS cells. Cells and contaminating bacteria were grown for 24 h at 37 °C under 5% CO_2. Next, cells were fixed, permeabilized, stained, and analyzed, following the procedure described above. Cellular monoculture studies in the absence of contaminating staphylococci were carried out as a control. All experiments were performed in triplicate with separately grown bacterial and cell cultures.

Phenotypic Polarization of Macrophages on Gold- and GNP-Coated Surfaces in the Absence and Presence of Contaminating Bacteria. Phenotypic polarization of murine macrophages in the direction of pro-inflammatory M1- or anti-inflammatory M2-phenotypes[38,39] was studied in the presence and absence of contaminating staphylococci and *E. coli* ATCC 25922 on smooth gold-, GNP-30/118-, and GNP-4/1101-coated surfaces. M1- and M2-macrophages can be distinguished by the presence of

https://dx.doi.org/10.1021/acsbiomaterials.9b01518
ACS Biomater. Sci. Eng. 2020, 6, 933−945

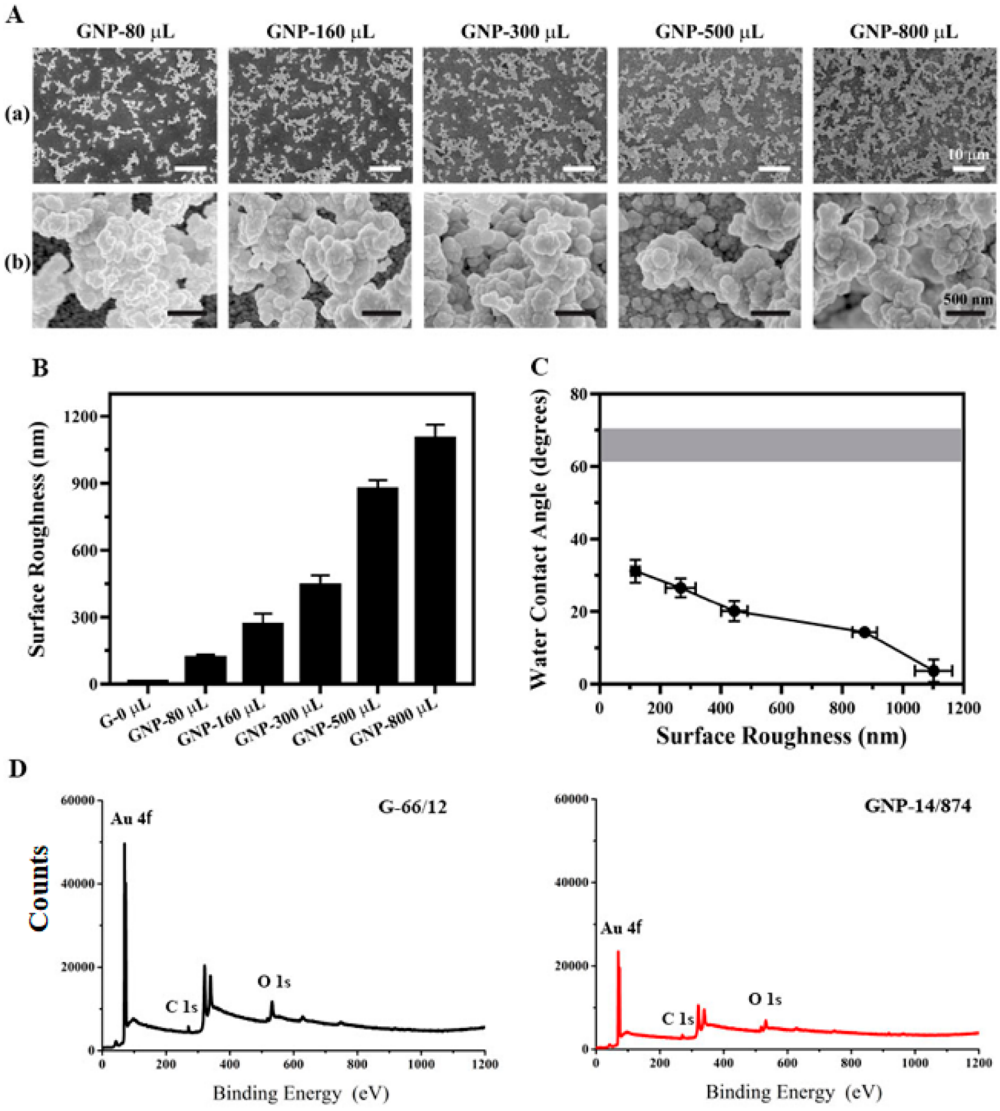

Figure 1. Characteristics of gold- and GNP-coated surfaces. (A) SEM micrographs of GNP-coated surfaces at low ((a)-row) and high ((b)-row) magnifications, prepared using different GNP-suspension volumes. (B) Surface roughnesses of gold- and GNP-coated surfaces prepared using different suspension volumes over an AFM evaluation length of 50 μm. Data are means ± standard deviation (SD), indicated by the error bars over three separately prepared samples. (C) Equilibrium water contact angles at room temperature as a function of the surface roughness. Data are means ± SD, indicated by the error bars over six separately prepared samples, while the gray band represents the average water contact angle, including its SD (bandwidth) for gold-coated silica wafers. (D) Examples of overall scans of electron binding energies found in XPS of smooth G-66/12 and nanostructured GNP-14/874 surfaces.

different transmembrane glycoproteins, of which Ym1 is unique to M2 phenotypic polarization in murine macrophages.[37,38] First, gold- and GNP-coated surfaces were placed in a 48-well plate, and 1 mL of bacterial suspension (1×10^3 bacteria per mL) was added for 1 h at room temperature, followed by rinsing 3 times with sterile PBS. Next, 2 mL of macrophages in suspension (3×10^4 per mL) in DMEM-HG was seeded in a 24-well plate with gold- or GNP-coated samples, with or without contaminating bacteria. After incubation at 37 °C under 5% CO_2 for 24 h, surfaces were rinsed with PBS and fixed with 3.7% paraformaldehyde in cytoskeleton stabilization buffer for 20 min. Fixed macrophages were permeabilized with 0.5% Triton X-100 in PBS for 3 min, and the nonspecific background was blocked with 5% BSA in PBS for 30 min. Fixed macrophages were incubated first in PBS with antibody Ym1 (goat-anti-mouse; 1% (v/v)) and BSA (1% (w/v) at room temperature for 1 h and washed 3 times with 1% BSA in PBS for 5 min. Subsequently, surfaces were stained with a second antibody (0.5% (v/v) donkey-anti-goat IgG for Ym1 labeled with TRITC) and 2 μg/mL phalloidin-FITC and washed 2 times with 1% BSA in PBS for 5 min, followed by a final rinse in PBS for 5 min. Macrophages with and without Ym1 expression appear green-fluorescent due to phalloidin-FITC staining upon excitation at 495 nm, but only murine macrophages expressing Ym1 appear red-fluorescent due to Ym1 antibody labeling upon excitation at 547 nm.[38,40,41] Five randomly selected images were taken on each surface, and all experiments were performed in triplicate with separately grown bacteria and macrophages.

Cytokine Secretion of Macrophages on Gold-Coated Surfaces in the Absence and Presence of Contaminating Bacteria. IL-10 and IL-12 secretion was determined as previously described.[42] Briefly, J774A.1 macrophages (1 mL, 10^5 cells/mL) were seeded in a 24-well plate on gold-coated samples and cultured in DMEM-HG for 48 h, followed by a 12 h starvation period in serum-free medium. Subsequently, samples were incubated in DMEM-HG for 24 h and exposed to different concentrations of bacterial suspensions in DMEM-HG medium supplemented with 24 mg/L gentamicin for 3 h, in order to avoid growth of bacteria. After washing with DMEM-HG, fresh medium was added, and samples were incubated for another 24 h. After 24 h, the supernatant was collected

https://dx.doi.org/10.1021/acsbiomaterials.9b01518
ACS Biomater. Sci. Eng. 2020, 6, 933−945

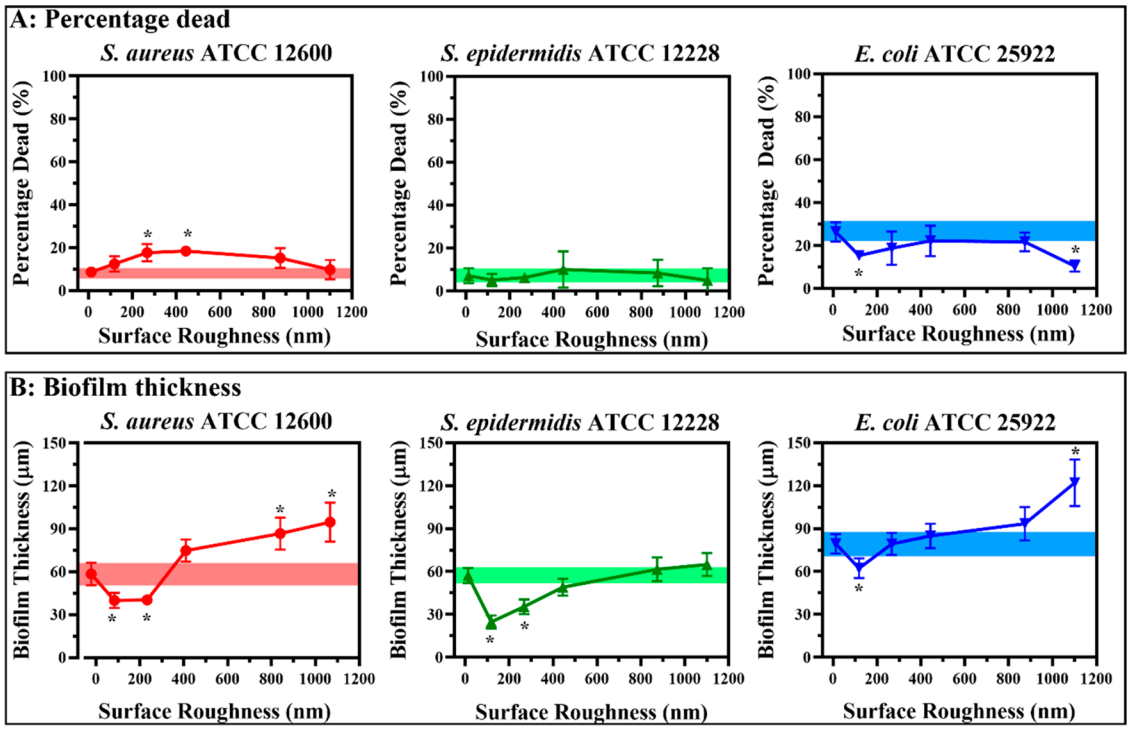

Figure 2. Viability of adhering staphylococci and *E. coli* and their biofilm thickness after 48 h growth. (A) The percentage of dead bacteria, determined from live/dead staining, adhering to different gold- and GNP-coated surfaces as a function of surface roughness. The colored bands represent the average percentage of dead bacteria, including its SD (bandwidth) on smooth G-66/12-coated silica wafers. (B) The biofilm thickness on different gold- and GNP-coated surfaces as a function of surface roughness. The colored bands represent the average thickness, including its SD (bandwidth) on smooth G-66/12-coated silica wafers. Data represent averages with error bars denoting SD over triplicate experiments with separately cultured bacteria and differently prepared samples. * indicates significant ($p < 0.05$) differences between GNP-coated surfaces and smooth G-66/12-coated silica wafers.

and stored at −20 °C for the enzyme-linked immunosorbent assay (ELISA). A Quantikine mouse IL-12 (R&D Systems, Minneapolis, MN, cat. M 1270) and a Quantikine Mouse IL-10 immunoassay kit (R&D Systems, Minneapolis, MN, cat. M 1000B) were used according to the manufacturer's instructions. The absorbance of the supernatant was measured at 450/570 nm using a microplate reader (FLUOstar OPTIMA, BMG labtech, Offenburg, Germany).

Tricultures of Tissue Cells, Macrophages, and Bacteria on Gold- and GNP-Coated Surfaces. Triculture experiments were performed with each of the three bacterial strains versus U2OS or hMS cells in the presence and absence of macrophages. Gold- and GNP-coated surfaces were placed in a 48-well plate, and 1 mL of bacterial suspension (1×10^3 per mL) was added for 1 h at room temperature. Next, wafers were rinsed 3 times with sterile PBS, and 2 mL of mixed suspension, containing 3×10^4 per mL macrophages and 1.5×10^4 per mL U2OS in modified growth medium (see above), was added for incubation at 37 °C, 5% CO_2 for 24 h. Next, cells were fixed, permeabilized, stained, and analyzed, following the procedure described above. All experiments were performed in triplicate with separately grown bacterial and cell cultures.

Statistical Analysis. All data are presented as a mean ± standard deviation (SD), and statistical comparisons were made using a one-way ANOVA test using Origin software. A p-value < 0.05 was considered statistically significant.

RESULTS

Surface Characterization of Gold Nanoparticle Coatings. GNP-coatings were prepared by sedimentation of different volumes of GNP-suspensions (GNP-diameter 100–150 nm) on gold-coated silica wafers. Scanning electron microscopy (SEM) images (Figure 1A) indicated that the density of GNPs at the silica wafer surface increased with increasing volume of the GNP-suspension, showing aggregation of GNPs for all suspension volumes applied. The surface roughnesses of the GNP-coated surfaces determined by AFM ranged from a nanoscale value of 12 nm for the gold-coated silica surface to a microscale value of 1100 nm for the highest GNP-suspension volume applied (Figure 1B).

Concurrent with increasing surface roughness, a decrease in water contact angles was found on the different GNP-coated surfaces that ranged from 30 degrees to 4 degrees depending on the GNP-suspension volume applied, while water contact angles on smooth gold-coated silica wafers amounted to 66 degrees (Figure 1C). Accordingly, gold- and GNP-coated surfaces were subsequently indicated by their hydrophilicity/roughness as G-66/12 (water contact angle 66 ± 4 degrees, surface roughness 12 ± 4 nm) for the smooth gold-coated surface or, e.g., GNP-30/118 (water contact angle 30 ± 4 degrees, surface roughness 118 ± 14 nm) for GNP-coated ones. Spectra of the photoelectron binding energies in all GNP-coated surfaces were similar (see Figure 1D for examples) with identical percentage compositions of carbon (38% ± 4), oxygen (13% ± 3), gold (42% ± 5), and nitrogen (2% ± 1), while corresponding percentages for G-66/12-coated silica wafers were 33%, 6%, 61%, and 0%, respectively.

Bacterial Adhesion and Biofilm Formation in Monoculture. Since the most distinguishing surface characteristic of the GNP-coated surfaces was their surface roughness, all data in the forthcoming parts of this Article will be graphically presented as a function of surface roughness. In order to evaluate whether GNP-coated surfaces had the potential to kill adhering bacteria, Gram-positive staphylococci and Gram-

https://dx.doi.org/10.1021/acsbiomaterials.9b01518
ACS Biomater. Sci. Eng. 2020, 6, 933–945

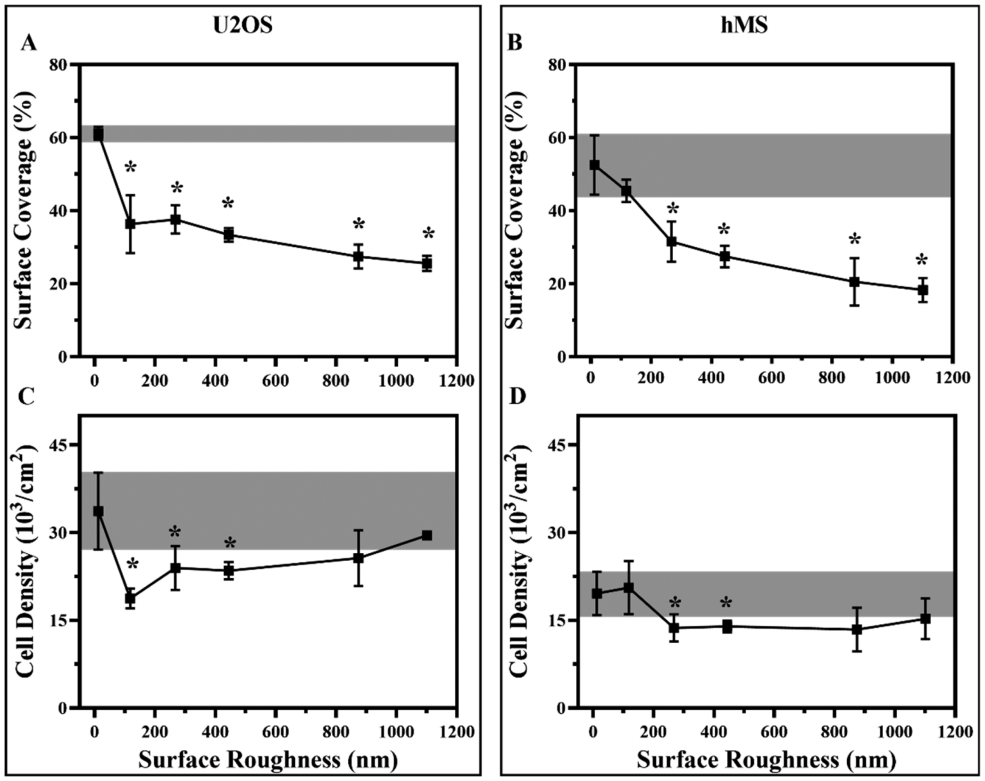

Figure 3. Cellular interactions to smooth G-66/12 and GNP-coatings after 24 h of growth. (A) Surface coverage by U2OS cells as a function of the surface roughness of the GNP-coated surfaces. The gray-shaded band represents the surface coverage on smooth G-66/12-coated surfaces. (B) Same as panel (A), now for hMS cells. (C) Number of U2OS cells per unit surface area as a function of the surface roughness of the GNP-coated surfaces. The gray-shaded band represents the cell number on smooth G-66/12-coated surfaces. (D) Same as panel (C), now for hMS cells. Data represent averages with error bars denoting SD over triplicate experiments with separately cultured bacteria and differently prepared samples. * indicates significant ($p < 0.05$) differences between GNP-coated surfaces and smooth G-66/12-coated silica wafers.

negative *E. coli* were allowed to sediment from suspension onto the different GNP-coatings during 3 h to a density of 1.0×10^6 bacteria per cm^2. Fluorescence microscopy after live/dead staining demonstrated a very low percentage of dead staphylococci and *E. coli* of less than 22% (Figure 2A), regardless of the hydrophilicity/roughness of the GNP-coating. More importantly, there was not one of the GNP-coated surfaces on which the percentage of dead bacteria for the three strains was significantly different from the one on a smooth G-66/12 surface. In a separate set of similar experiments, the adhering bacteria were allowed to grow into a biofilm by replacing the buffer above the samples with growth medium, and after 48 h of growth, the resulting biofilm thickness was measured using OCT (see Figure 2B). Biofilm thickness of all three strains increased with increasing surface roughness. However, the thickness of *S. aureus* biofilms on GNP-coated surfaces was smaller than on smooth G-66/12 surfaces up to GNP-21/444 coatings and only exceeded the biofilm thickness on smooth G-66/12 surfaces when the surface hydrophilicity/roughness increased to above 21 degrees/444 nm (Figure 2B). *S. epidermidis* biofilms on smooth G-66/12 surfaces were of equal thickness than *S. aureus* biofilm, also demonstrating a smaller thickness up to GNP-21/444-coated surfaces, but for *S. epidermidis* the thickness on the roughest GNP-4/1101 surface did not exceed the thickness on smooth G-66/12 surfaces. *E. coli* biofilms were generally thicker than *S. aureus* ones, most notably on the smooth G-66/12 surface. A significant ($p < 0.05$) increase in biofilm thickness for the Gram-negative pathogen started only above a hydrophilicity/roughness of 14/874 nm.

Cytotoxicity, Cellular Adhesion, and Spreading in Monoculture. Fluorescence images of phalloidin-FITC/DAPI stained, human osteosarcoma (U2OS; Figure S1A) and human mesenchymal stem cells (hMS; Figure S1B) after 24 h of growth on smooth G-66/12-coated and two GNP-coated surfaces in the absence of contaminating bacteria show good spreading of both cell lines on all surfaces, with generally more cells present on smooth G-66/12-coated silica surfaces than on the GNP-coated ones. Surface coverage of smooth G-66/12 coatings was fairly low between 40 and 60% depending on the cell line considered and showed a gradual decrease with increasing roughness of the GNP-coatings (Figure 3A and 3B). The low surface coverage was not caused by cytotoxicity of the GNP-coatings. The absence of cytotoxicity of GNP-coatings was confirmed using the CCK-8 assay, as shown in Figure S2. The relative viability was similar on tissue-culture polystyrene ("blank"), smooth G-66/12-coated, and nanostructured GNP-coated surfaces, indicating good biocompatibility. Cell numbers, on the other hand, showed an incidental minor decrease on specific GNP-coatings for U2OS cells (Figure 3C), but hMS cell numbers remained the same as on smooth G-66/12 coatings for all GNP coatings (Figure 3D).

Cellular Adhesion and Spreading in Biculture with Contaminating Bacteria. The presence of a low number of adhering *S. aureus* (250 cm^{-2}, representing a biomaterial surface contamination level equal as found in per-operative contamination[37]) had a detrimental effect on the adhering

https://dx.doi.org/10.1021/acsbiomaterials.9b01518
ACS Biomater. Sci. Eng. 2020, 6, 933−945

cells. Green-fluorescence due to the cytoskeleton disappeared, while the confined blue-fluorescence of the nuclei as observed in the absence of bacterial contamination appeared smeared out over much larger areas than observed in the absence of *S. aureus* (Figure S1). The presence of contaminating *S. epidermidis* and of *E. coli* on GNP-30/118-coated surfaces neither caused the disappearance of cytoskeleton green-fluorescence nor extensive smearing of the blue-fluorescence.

Accordingly, the surface coverage and number of adhering U2OS and hMS cells were further analyzed in the presence of contaminating *S. epidermidis* and *E. coli*, since these parameters have been suggested to be predictive for the outcome of the race for the surface between bacterial colonization and tissue integration and therewith for the ultimate fate of a biomaterials implant or device in the human body.[23,43] No such quantitative data could be extracted in the case of contaminating *S. aureus*, due to the absence of cytoskeleton green-fluorescence and the extent of blue-fluorescence smearing.

In the presence of contaminating *S. epidermidis*, surface coverage of both cell types on the smooth G-66/12 coating remained similarly high as in the absence of contaminating staphylococci (compare Figure 4 and Figure 3). Upon increasing the roughness of the GNP-coatings, the presence of contaminating *S. epidermidis* gradually decreased tissue coverage, as it did in the absence of staphylococci. Cell number per unit area was essentially the same on all GNP-coatings in the absence and presence of contaminating staphylococci (also compare Figure 4 and Figure 3), indicating that the decrease in tissue coverage was due to a decrease in spreading of individual cells and not a decrease in the numbers of adhering cells. In the presence of contaminating *E. coli* however, tissue coverage on smooth G-66/12 coatings reduced severely to less than 10% for both U2OS and hMS cells. Different than in the presence of contaminating *S. epidermidis*, tissue coverage by U2OS and hMS cells in the presence of contaminating *E. coli* showed a small maximum of around 20% on GNP-coatings with a hydrophilicity/roughness around 30/118 followed by a gradual decrease with increasing roughness, concurrent with a decrease in cell number (Figure 4).

Macrophage Polarization in Bicultures with Bacteria. In order to determine whether macrophage polarization on the different surfaces could be responsible for possible beneficial effects on cellular interaction with GNP-30/118- and GNP-4/1101-coatings, biculture studies were done, identifying murine macrophage polarization on bacterially contaminated surfaces based on the presence of Ym1, a transmembrane glycoprotein[40,41] (see Figure S3 for an example). Ym1 is described as uniquely occurring in murine M2-macrophages and not in murine M1-macrophages.[40,41]

Very few macrophages on smooth gold- and GNP-coated surfaces in the absence of contaminating bacteria possessed Ym1 transmembrane glycoprotein, but in the presence of bacterial contamination on the surface nearly all macrophages expressed Ym1 (Figure 5). This suggests that M1/M2 macrophage polarization is not responsible for possible beneficial effects of different GNP coatings in the race for the surface between tissue cells and contaminating bacteria.

Impact of Macrophages on the Race for the Surface between Cellular Interaction and Bacterial Colonization in Tricultures. Whereas in the above section, the race for the surface has been mimicked in bicultures of tissue cells and bacteria, clinically the true race for the surface in the human body occurs in the presence of macrophages. Therefore,

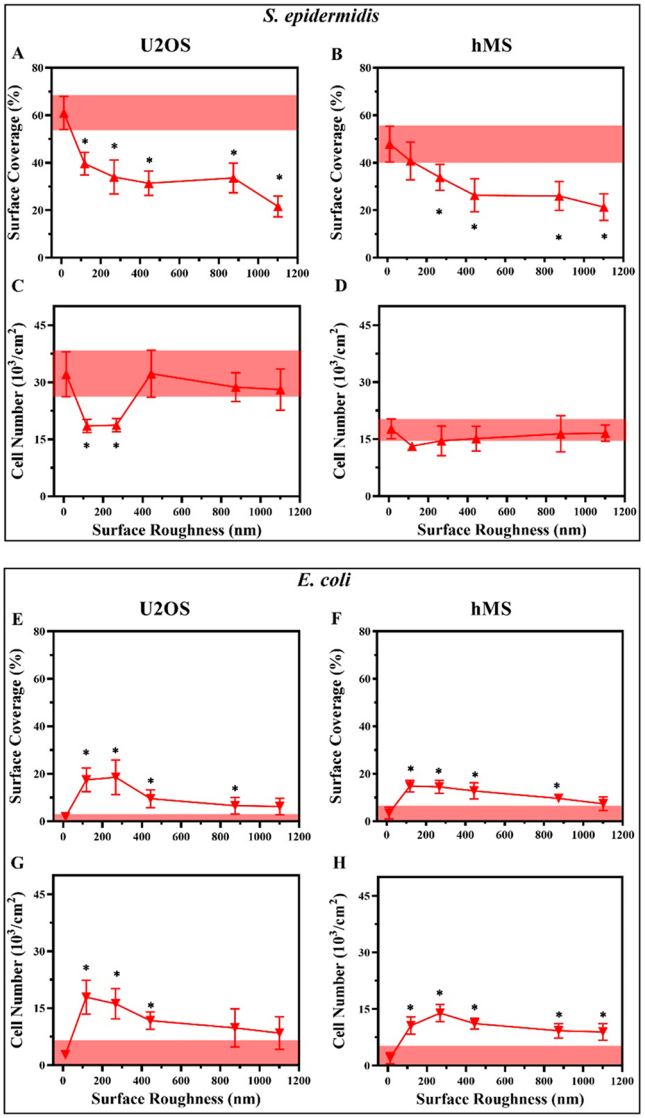

Figure 4. Surface coverage and cell number per unit area on bacterially contaminated smooth G-66/12 and GNP-coatings after 24 h of growth. (A) Surface coverage by U2OS cells as a function of the surface roughness on *S. epidermidis* contaminated GNP-coated surfaces. The red-shaded band represents the surface coverage on smooth G-66/12-coated surfaces. (B) Same as panel (A), now for hMS cells. (C) Number of U2OS cells per unit surface area as a function of the surface roughness on *S. epidermidis* contaminated GNP-coated surfaces. The red-shaded band represents the cell number on bacterially contaminated, smooth G-66/12-coated surfaces. (D) Same as panel (C), now for hMS cells. (E), (F), (G), and (H) same as panels (A), (B), (C), and (D) respectively, but now for *E. coli*. Data represent averages with error bars denoting SD over triplicate experiments with separately cultured bacteria and differently prepared samples. * indicates significant ($p < 0.05$) differences between GNP-coated surfaces and smooth G-66/12-coated silica wafers.

triculture studies were performed as well on smooth G-66/12-coated and two selected GNP-coated surfaces. In triculture studies, macrophages were introduced together with U2OS or hMS cells, and surface coverage by cells was evaluated in the presence of adhering, contaminating staphylococci and *E. coli* (Table 1 and Figure S4). Whereas cells showed no cytoskeleton green-fluorescence and blue-fluorescence smearing in the presence of contaminating *S. aureus*, addition of

https://dx.doi.org/10.1021/acsbiomaterials.9b01518
ACS Biomater. Sci. Eng. 2020, 6, 933−945

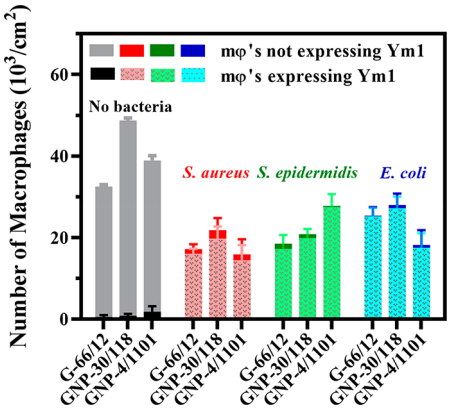

Figure 5. Numbers of murine macrophage (mφ) (not) expressing Ym1 transmembrane glycoprotein on smooth gold- and GNP-coated surfaces in the absence and presence of bacterial contamination (250 bacteria cm^{-2}) with *S. aureus* ATCC 12600, *S. epidermidis* ATCC 12228, and *E. coli* ATCC 25922. Data represent averages with error bars denoting SD over triplicate experiments with separately cultured bacteria and macrophages and differently prepared samples.

macrophages restored the combination of green- and confined blue-fluorescence staining to allow quantification of the surface coverage by cells (Table 1) and the number of adhering cells per unit area (Table 2). Beneficial effects of macrophage presence were strongest on the GNP-30/118-coating and in triculture experiments comprising adhering, contaminating Gram-positive staphylococci. In tricultures with adhering *S. epidermidis*, the presence of macrophages stimulated the surface coverage and number of adhering cells to levels higher than observed on the smooth G-66/12-coating in the absence of contaminating bacteria. Macrophages aided neither U2OS nor hMS cells in their race for the surface against contaminating Gram-negative *E. coli* and surface coverages, and cell numbers were similar in the absence and presence of macrophages.

DISCUSSION

In this paper, mono-, bi-, and triculture studies were carried out to determine whether macrophages are stimulated on smooth gold- and GNP-coated surfaces to polarize toward their M1- or M2-phenotype and how they influence the race for the surface[23] between bacteria and tissue cells attempting to integrate a surface. Uniquely, experiments were done in the absence and presence of contaminating bacteria adhering on these coatings in low numbers, as often per-operatively introduced during biomaterial implant surgery. Although the distinction between M1- and M2-macrophages encompasses a spectrum of phenotypes,[44] it is safe to conclude from that data that murine macrophages in monoculture tended toward their pro-inflammatory "fighting" M1-phenotype on all gold- and GNP-coated surfaces to combat the presence of the biomaterial. However, in bicultures in the presence of a bacterially contaminated biomaterial, the macrophages adapted an important feature (Ym1 expression) of their anti-inflammatory "fix-and-repair" M2-phenotype, regardless of the type of coating involved (Figure 5). This yields the conclusion that macrophages prefer, in a first instance, to fix and repair potential damage done to tissue cells by adhering, contaminating bacteria rather than fighting the presence of the biomaterial or the contaminating bacteria as a potential cause of tissue damage. The preference of macrophages to fix-and-repair in tricultures may be one of the reasons why biomaterial-associated infections are hard to eradicate by the host-immune system. Keeping macrophages in their pro-inflammatory M1-phenotype to fight contaminating bacteria on a biomaterial surface might prevent lingering infections and therewith long-lasting troublesome episodes for patients relying on biomaterials implants or devices for their quality of life. However, although the fighting M1-phenotype might be helpful to eradicate biomaterial-associated infection, the prolonged presence of M1-macrophages at the same time also bears the risk of causing collateral tissue damage (fibrotic disease).[45] Thus, while the M2-phenotype of macrophages on GNP-coated surfaces in the presence of bacterial contamination may be considered beneficial for tissue integration, a slightly longer episode during which macrophages would adapt their pro-inflammatory M1-phenotype immediately after implantation would be desirable to prevent biomaterial-associated infection. Possibly the porosity of the GNP-coatings might be used to absorb and release drugs such as interferon γ in combination with lipopolysaccharides or tumors necrosis factor α to keep macrophages longer in their M1-phenotype.[46] In order to prevent the occurrence of fibrotic diseases, loading of such a release system should be limited to confine the duration during

Table 1. Surface Coverage (%) by U2OS or hMS Cells on Bacterially Contaminated Surfaces (250 Bacteria Adhering cm^{-2}) in the Absence or Presence of J774.A1 Murine Macrophages (mφ)[e]

culture type		smooth G-66/12		GNP-30/118		GNP-4/1101	
U2OS in monoculture		61 ± 2		36 ± 8[d]		25 ± 2[d]	
hMS in monoculture		52 ± 8		45 ± 3		18 ± 3[d]	
presence of bacteria in bi- or tricultures		biculture	triculture with mφ	biculture	triculture with mφ	biculture	triculture with mφ
S. aureus ATCC 12600	U2OS	ND[a]	2.4 ± 1.3[c,d]	ND[a]	4.0 ± 0.3[c,d]	ND[a]	0.8 ± 0.4[c,d]
	hMS	ND[a]	5.0 ± 1.3[c,d]	ND[a]	11.7 ± 3.0[c,d]	ND[a]	7.6 ± 0.7[c,d]
S. epidermidis ATCC 12228	U2OS	61 ± 7	70 ± 6[b]	40 ± 5[d]	69 ± 2[b,c]	22 ± 4[d]	30 ± 6[d]
	hMS	48 ± 8	50 ± 4	40 ± 8	61 ± 3[b,c,d]	21 ± 6[d]	43 ± 1[b,c,d]
E. coli ATCC 25922	U2OS	1.9 ± 1.2[b,d]	1.6 ± 1.2[b,d]	17.4 ± 5.0[b,d]	18.2 ± 6.3[b,d]	6.2 ± 3.5[b,d]	7.8 ± 2.9[b,d]
	hMS	3.5 ± 2.5[b,d]	6.5 ± 1.5[b,d]	14.8 ± 2.5[b,d]	14.5 ± 1.4[b,d]	7.4 ± 2.9[b,d]	6.0 ± 0.6[b,d]

[a]Not determined due to nucleus disintegration in the presence of *S. aureus*. [b]Significantly ($p < 0.05$) different from the corresponding monoculture data. [c]Significantly ($p < 0.05$) different from the corresponding biculture data. [d]Significantly ($p < 0.05$) different from the corresponding smooth gold-coated data. [e]Monoculture studies comprised only U2OS or hMS cells, while experiments on surfaces with contaminating staphylococci or *E. coli* are indicated as biculture studies, and triculture studies are done in the additional presence of macrophages next to contaminating bacteria and tissue cells. See Supporting Information Figure S4 for corresponding fluorescence images of triculture data. Data represent averages with ± signs denoting SD over triplicate experiments with separately cultured cells and bacteria and differently prepared samples.

https://dx.doi.org/10.1021/acsbiomaterials.9b01518
ACS Biomater. Sci. Eng. 2020, 6, 933−945

Table 2. Analogue Table of Table 1, Summarizing the Cell Number per Unit Area (10^3/cm^2) of U2OS or hMS Cells on Bacterially Contaminated Surfaces in the Absence or Presence of J774.A1 Murine Macrophages (mφ)[c]

culture type		smooth G-66/12		GNP-30/118		GNP-4/1101	
U2OS in monoculture		34 ± 7		19 ± 2		30 ± 1	
hMS in monoculture		20 ± 4		21 ± 5		15 ± 4	
presence of bacteria in bi- or tricultures		biculture	triculture with mφ	biculture	triculture with mφ	biculture	triculture with mφ
S. aureus ATCC 12600	U2OS	ND[a]	1.4 ± 1.1	ND[a]	4.9 ± 1.3[b]	ND[a]	1.2 ± 0.7
	hMS	ND[a]	7.6 ± 1.7	ND[a]	22.1 ± 3.4	ND[a]	9.8 ± 2.1
S. epidermidis ATCC 12228	U2OS	32.1 ± 5.9	28.4 ± 7.2	18.5 ± 1.7	25.9 ± 7.8	28.1 ± 5.4	19.2 ± 1.1
	hMS	28.4 ± 7.0	12.2 ± 1.8	13.2 ± 0.9	15.9 ± 1.2	13.6 ± 2.1	12.7 ± 3.2[b]
E. coli ATCC 25922	U2OS	2.8 ± 0.4[b]	12.8 ± 6.5	17.9 ± 4.5	16.1 ± 1.5	8.5 ± 4.3	16.1 ± 1.2
	hMS	2.0 ± 1.5	4.5 ± 1.5	10.6 ± 2.3	16.3 ± 1.2	8.3 ± 2.2	6.0 ± 0.7

[a]Not determined due to nucleus disintegration in the presence of *S. aureus*. [b]Significantly ($p < 0.05$) different from the corresponding smooth gold-coated data. [c]Monoculture studies comprised only U2OS or hMS Cells, while experiments on surfaces with contaminating staphylococci or *E. coli* are indicated as biculture studies, and triculture studies are done in the additional presence of macrophages next to contaminating bacteria and tissue cells. See Supporting Information Figure S4 for corresponding fluorescence images of triculture data. Data represent averages with ± signs denoting SD over triplicate experiments with separately cultured cells and bacteria and differently prepared samples.

which macrophages are kept in their pro-inflammatory fighting M1-phenotype. Once contaminating bacteria are eradicated, the risk of biomaterial-associated infection due to per-operative contamination is reduced, and macrophages can polarize in specialized anti-inflammatory M2-subphenotypes[44] to help tissue cells overcome possible damage they may have suffered due to the presence of a bacterially contaminated biomaterial implant.

Macrophage polarization on biomaterial surfaces has been studied predominantly with respect to the foreign body reaction but not in the presence of low numbers of bacteria, contaminating a biomaterial implant surface. Our study on macrophage polarization focuses on the modulation of macrophage polarization in the presence of a biomaterial, contaminated with a low number of adhering bacteria, as often per-operatively introduced during biomaterial implant surgery. Macrophages all tended toward their pro-inflammatory M1-phenotype in the absence of contaminating bacteria on all GNP-coated surfaces, regardless of their hydrophilicity/roughness. Also, on titanium surfaces with roughnesses between 0.09 and 1.44 μm, macrophage polarization toward the M1-phenotype was seen.[47] On the other hand, extremely hydrophilic (full spreading of water) titanium surfaces with roughnesses ranging between 0.6 to 3.5 μm showed higher percentages of M2-phenotypes than more smooth hydrophobic titanium surfaces (more than 90 deg water contact angle).[48] Also, nanopatterned metallic glasses modulated macrophage responses toward their M2-phenotype.[49] However, macrophage polarization is modulated not only by the presence of a biomaterial but also by bacteria. Planktonic *S. aureus* in suspension (i.e., not adhering on a biomaterial)[50,51] or after *in vivo* injection in the peripheral blood of rats,[51] both in the absence of a biomaterial, stimulated macrophage polarization into their M2-phenotype. Other studies indicated that the Gram-character of planktonic bacteria in the absence of a biomaterial, impacted macrophage polarization based on cytokine secretion.[42] However, exposure to most strains resulted in either high or low secretion levels of IL-10 and IL-12, rather than a clear M1 or M2 profile. In general, the Gram-negative strains such as *E. coli* induced higher levels of cytokine secretion compared to the Gram-positive strains.

In several routine literature assays[42,52] to study macrophage polarization based on cytokine secretion, macrophages are grown on a substratum surface and directly exposed to high numbers of bacteria (Figure 6A). This is different than in the case of macrophages in biculture on a substratum surface

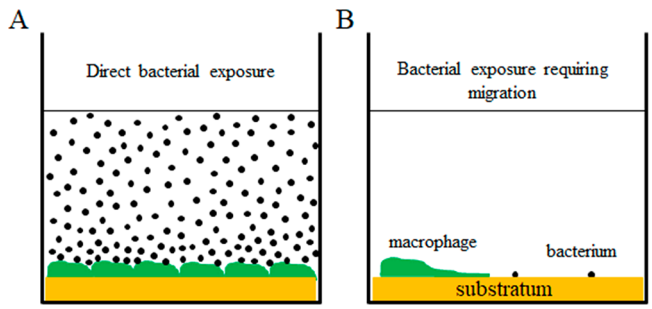

Figure 6. (A) In a routine assay to study macrophage polarization, a macrophage covered substratum surface is directly exposed to high numbers of bacteria.[51] (B) Macrophages on a biomaterial surface contaminated with a low number of adhering bacteria, as used in this study, have to migrate over considerable distances to reach an adhering bacterium.

contaminated with low numbers of contaminating bacteria (Figure 6B). On a bacterially contaminated surface, macrophages have to migrate considerable distances over a substratum surface before they encounter a contaminating bacterium (see also Figure 6B). Accordingly, we have attempted to relate IL-10 and IL-12 secretion with Ym1 expression in macrophages directly exposed to low numbers of contaminating bacteria according to Figure 6B. These attempts failed, most likely because cytokine secretion was too low for quantification.

Therefore, we also carried out experiments to relate IL-10 and IL-12 secretion with Ym1 expression in macrophages directly exposed to bacteria according to Figure 6A. IL-10 and IL-12 secretion depended strongly on the number of bacteria involved in the assay (Figure S5), confirming the above suggestion that cytokine secretion may be too low for quantification in case low numbers of bacteria are involved. In line with the literature,[42] IL-10 secretion depended on the bacterial strain involved and was absent during direct exposure to *S. aureus*, while slightly increasing during exposure to *S. epidermidis* suspensions with more than 10^7 bacteria per mL. As also observed by Christofferson et al.,[42] direct exposure to *E. coli* gave clear secretion of IL-10 also at low concentrations. For all strains, IL-12 secretion remained below detection.

https://dx.doi.org/10.1021/acsbiomaterials.9b01518
ACS Biomater. Sci. Eng. 2020, 6, 933−945

Importantly, for *S. epidermidis* and *E. coli*, increased IL-10 secretion corresponded with expression of Ym1.

Accordingly, this study is the first to demonstrate macrophage polarization on bacterially contaminated surfaces, as relevant with respect to the occurrence of biomaterial-associated infection after biomaterial implant surgery. It shows a preference of murine macrophages to fix-and-repair in their anti-inflammatory M2-phenotype rather than to (first) fight contaminating bacteria on a biomaterial surface in their pro-inflammatory M1-phenotype, based on Ym1 expression, the key-marker of the M2-phenotype in murine macrophages.[40,41] Possibly, increased Ym1 expression must possibly be considered as a first step toward the M2-phenotype, as it only corresponded in direct exposure assays with IL-10 secretion for two out of the three bacterial strains involved in this study, in the absence of detectable IL-12 secretion. This suggestion is confirmed by studies in which macrophage polarization was studied in the presence of a full-grown biofilm on a biomaterial surface, facilitating simultaneous contact of macrophages with a multitude of bacteria. In full-grown biofilm studies, increased expression of anti-inflammatory markers such as arginase-1, IL-4, and IL-10 was indeed found.[52] Also macrophages invading *S. aureus* biofilms displayed gene-expression indicative of the M2-phenotypes.[53] Unlike direct exposure, studies with planktonic bacteria and macrophages have shown[42] the Gram-character of bacteria low-level adhering to different GNP-coated surfaces did not impact Ym1 expression.

The actual aid provided in their anti-inflammatory M2-phenotype by macrophages to support tissue integration of bacterially contaminated biomaterial surfaces did depend on the bacterial strain involved, more specifically its virulence. Moreover, these coculture studies yielded a bacterial strain dependent disappearance of cytoskeleton green-fluorescence in combination with smearing of the blue-fluorescence, caused by *S. aureus* and *E. coli* on G-66/12- and GNP-4/1101-coated surfaces but not by *S. epidermidis* and *E. coli* on GNP-30/118-coated surfaces. The absence of cytoskeleton green-fluorescence likely indicates cell detachment, especially by highly virulent Gram-positive *S. aureus*.[32] Accordingly, *S. aureus* completely impeded tissue cell coverage on both smooth G-66/12 and GNP-30/118 coatings (Table 1), and macrophages provided clear help in cell spreading over the biomaterial surface. Although cell spreading on *S. aureus* contaminated surfaces remained low in the presence of macrophages, it was quantifiable from a restored combination of green cytoskeleton fluorescence and confined blue nucleus fluorescence. Cell spreading on *S. aureus* contaminated surfaces in the presence of macrophages was maximal on GNP-30/118 coatings, especially in the case of hMS cells. Similarly, cell spreading over coatings contaminated with Gram-positive *S. epidermidis*, i.e., considered the least virulent of the three strains involved, was increased in the presence of M2-phenotype macrophages, and effects were most notable for both U2OS and hMS cells on GNP-30/118 coatings. M2-phenotypic macrophages did not provide significant aid to either cell line in integrating GNP-coatings contaminated with Gram-negative *E. coli*. Thus, whereas we show that opposite to planktonic bacterial presence, macrophage polarization in the presence of bacteria adhering to a biomaterial surface is not impacted by the Gram-character of the bacteria, the absence of effective aid to tissue cell by M2-macrophages in the presence of Gram-negative *E. coli* in comparison with Gram-positive staphylococci suggests that the Gram-character of adhering, contaminating bacteria may impact possibly further polarization in specialized M2-subphenotypes.

The above conclusions are highly new and could only be drawn from triculture studies. Triculture studies are uniquely opposed to monoculture studies and clearly bear a larger clinical significance. Monoculture studies have been carried out on nanostructured biomaterials before with bacteria,[46,47] tissue cells,[47,48,54] and macrophages,[17−20] but extrapolation of monoculture results toward the clinically more relevant race for the surface is impossible. Moreover, their results are hard to compare with ours, if only because the term "nanostructured" can refer to highly different types of surfaces. The GNP-coated surfaces in this study are made of relatively hydrophobic gold nanoparticles, but due to their aggregation, the roughness of the resulting surfaces does not really fall in the nanoscale. Moreover, nanostructured surfaces can possess a random roughness, as ours, or a periodic roughness, such as nanopillared ones.[11,12,55] Nanoscale contact induced bacterial cell death was confirmed for a *S. aureus* strain in contact with highly periodically occurring nanopillars.[11,12,14] Likely, the roughness of our GNP-coated surfaces was too high to yield nanoscale contact with its high local stresses exerted on the bacterial cell wall held responsible for bacterial cell death.[11,12] In monoculture, neither individual U2OS nor hMS cells liked to spread on the rougher GNP-coated surfaces, whereas hMS cells also grew in lower numbers than the U2OS cells. Possibly, this is due to a mismatch between typical cell surface features involved in their adhesion with the submicron- and micron-scale roughness created on our GNP-coated surfaces,[56,57] as also suggested for embryonic stem cells.[35]

In many studies, hydrophobicity is varied by changing the surface chemistry,[58] while it cannot be excluded that a specific chemistry will be more determinant for the tissue cell response than hydrophobicity as a nonspecific property. An advantage of our GNP-coated surfaces is that they all carry the same chemical surface composition determined by XPS, and therewith the influence of surface chemistry can be excluded in our results, although as a price to pay for this, hydrophilicity and roughness varied in concert with each other (Figure 1). Both U2OS and hMS showed a limited surface coverage on relatively hydrophobic gold surfaces, which is in line with the general preference of tissue cells to adhere and spread better on more hydrophilic surfaces.[59,60] Although the GNP-coated surfaces manifested themselves as more hydrophilic than smooth gold surfaces, cells did not like to grow and spread on these rougher and accordingly more hydrophilic coatings. This is because the manifestation of increased hydrophilicity is due to capillary suction of water through the nanostructures, causing a lower water contact angle on nanostructured surfaces while the intrinsic surface remains equally hydrophobic as smooth gold. It is the intrinsic hydrophobicity of the gold nanoparticles that the cells do not like, and hence they show less surface integration. Therewith monoculture studies would have yielded the erroneous conclusion that GNP-coated surfaces carry no benefits with respect to cellular interactions, while through the use of tricultures we have been able to point to a clear advantage of specific GNP-coatings with respect to the race for the surface and therewith the aid of a bacterially contaminated biomaterials implant.

https://dx.doi.org/10.1021/acsbiomaterials.9b01518
ACS Biomater. Sci. Eng. 2020, 6, 933−945

CONCLUSIONS

Murine macrophages in monoculture on all gold- and GNP-coated surfaces demonstrated no Ym1 expression as one of the most important features of their pro-inflammatory "fighting" M1-phenotype to combat the biomaterial. However, in bicultures with low-level adhering, contaminating bacteria, macrophages expressed Ym1 in high numbers indicative in murine macrophages for a phenotype that tends toward the anti-inflammatory "fix-and-repair" M2-phenotype. Damage repair of cells by macrophages improved cell adhesion and spreading especially on GNP-30/118 coatings in the presence of contaminating Gram-positive staphylococci but provided little aid when surfaces were contaminated with adhering Gram-negative *E. coli*. Thus, the merits on GNP-coatings to prevent biomaterial-associated infection critically depend on the hydrophilicity/roughness of the coatings and the virulence of the contaminating bacterial strain. The ease of fabricating these randomly structured, GNP-coatings provides a clear benefit for their use as a more infection-resistant biomaterial coating than established by smooth surfaces.

ASSOCIATED CONTENT

Supporting Information

The Supporting Information is available free of charge at https://pubs.acs.org/doi/10.1021/acsbiomaterials.9b01518.

Additional figures, including cytotoxicity of different cell types on gold and GNP-coated surfaces, fluorescence images of different cell types on gold- and GNP-coated surfaces, fluorescence images of murine macrophage polarization on gold and GNP-coated surfaces in absence/presence of low-level adhering bacteria, fluorescence images of different cell types on low-level, bacterially contaminated gold- and GNP-coated surfaces in presence of macrophages and macrophages expressing Ym1 and IL-10 growing on substratum surface and exposed to different concentrations of bacterial suspension (PDF)

AUTHOR INFORMATION

Corresponding Authors

Henny C. van der Mei − *University of Groningen, University Medical center Groningen, Department of Biomedical Engineering, 9713 AV Groningen, The Netherlands;* orcid.org/0000-0003-0760-8900; Email: h.c.van.der.mei@umcg.nl

Hong Chen − *College of Chemistry, Chemical Engineering and Materials Science, Soochow University, Suzhou 215123, P. R. China;* orcid.org/0000-0001-7799-4961; Email: chenh@suda.edu.cn

Authors

Yafei Luan − *College of Chemistry, Chemical Engineering and Materials Science, Soochow University, Suzhou 215123, P. R. China; University of Groningen, University Medical center Groningen, Department of Biomedical Engineering, 9713 AV Groningen, The Netherlands*

Melissa Dijk − *University of Groningen, University Medical center Groningen, Department of Orthodontics, 9713 GZ Groningen, The Netherlands*

Gésinda I. Geertsema-Doornbusch − *University of Groningen, University Medical center Groningen, Department of Biomedical Engineering, 9713 AV Groningen, The Netherlands*

Jelly Atema-Smit − *University of Groningen, University Medical center Groningen, Department of Biomedical Engineering, 9713 AV Groningen, The Netherlands*

Yijin Ren − *University of Groningen, University Medical center Groningen, Department of Orthodontics, 9713 GZ Groningen, The Netherlands*

Henk J. Busscher − *University of Groningen, University Medical center Groningen, Department of Biomedical Engineering, 9713 AV Groningen, The Netherlands*

Complete contact information is available at: https://pubs.acs.org/10.1021/acsbiomaterials.9b01518

Notes

The authors declare the following competing financial interest(s): H.J.B. is also director-owner of a consulting company, SASA BV. The authors declare no potential conflicts of interest with respect to authorship and/or publication of this article.

ACKNOWLEDGMENTS

This work was financially supported by the National Key Research and Development Program of China (2016YFC1100402), the National Natural Science Foundation of China (21334004), and UMCG, Groningen, The Netherlands.

REFERENCES

(1) Darouiche, R. O. Treatment of Infections Associated with Surgical Implants. *N. Engl. J. Med.* **2004**, *350*, 1422−1429.

(2) Busscher, H. J.; Ploeg, R. J.; Van der Mei, H. C. Snapshot: Biofilms and Biomaterials; Mechanisms of Medical Device Related Infections. *Biomaterials* **2009**, *30*, 4247−4248.

(3) Campoccia, D.; Montanaro, L.; Arciola, C. R. A Review of the Clinical Implications of Anti-Infective Biomaterials and Infection-Resistant Surfaces. *Biomaterials* **2013**, *34*, 8018−8029.

(4) Zaat, S. A. J.; Broekhuizen, C. A. N.; Riool, M. Host Tissue as A Niche for Biomaterial-Associated Infection. *Future Microbiol.* **2010**, *5*, 1149−1151.

(5) Grainger, D. W.; Van der Mei, H. C.; Jutte, P. C.; Van den Dungen, J. J. A. M.; Schultz, M. J.; Van der Laan, B. F. A. M.; Zaat, S. A. J.; Busscher, H. J. Critical Factors in the Translation of Improved Antimicrobial Strategies for Medical Implants and Devices. *Biomaterials* **2013**, *34*, 9237−9243.

(6) Ziebuhr, W.; Hennig, S.; Eckart, M.; Kranzler, H.; Batzilla, C.; Kozitskaya, S. Nosocomial Infections by *Staphylococcus epidermidis*: How a Commensal Bacterium Turns into a Pathogen. *Int. J. Antimicrob. Agents* **2006**, *28* (Suppl 1), 14−20.

(7) Tande, A. J.; Patel, R. Prosthetic Joint Infection. *Clin. Microbiol. Rev.* **2014**, *27*, 302−345.

(8) Pääkkönen, M.; Kallio, M. J.; Kallio, P. E.; Peltola, H. Sensitivity of Erythrocyte Sedimentation Rate and C-Reactive Protein in Childhood Bone and Joint Infections. *Clin. Orthop. Relat. Res.* **2010**, *468*, 861−866.

(9) Hasan, J.; Crawford, R. J.; Ivanova, E. P. Antibacterial Surfaces: the Quest for a New Generation of Biomaterials. *Trends Biotechnol.* **2013**, *31*, 295−304.

(10) Tian, J.; Zhao, Z.; Kumar, A.; Boughton, R. I.; Liu, H. Recent Progress in Design, Synthesis, and Applications of One-Dimensional TiO_2 Nanostructured Surface Heterostructures: A Review. *Chem. Soc. Rev.* **2014**, *43*, 6920−6937.

(11) Hizal, F.; Choi, C. H.; Busscher, H. J.; Van der Mei, H. C. Staphylococcal Adhesion, Detachment and Transmission on Nanopillared Si Surfaces. *ACS Appl. Mater. Interfaces* **2016**, *8*, 30430−30439.

(12) Svensson, S.; Forsberg, M.; Hulander, M.; Vazirisani, F.; Palmquist, A.; Lausmaa, J.; Thomsen, P.; Trobos, M. Role of

Nanostructured Gold Surfaces on Monocyte Activation and *Staphylococcus epidermidis* Biofilm Formation. *Int. J. Nanomed.* **2014**, *9*, 775−794.
(13) Pham, V. T. H.; Truong, V. K.; Orlowska, A.; Ghanaati, S.; Barbeck, M.; Booms, P.; Fulcher, A. J.; Bhadra, C. M.; Buividas, R.; Baulin, V.; Kirkpatrick, C. J.; Doran, P.; Mainwaring, D. E.; Juodkazis, S.; Crawford, R. J.; Ivanova, E. P. "Race for the Surface": Eukaryotic Cells Can Win. *ACS Appl. Mater. Interfaces* **2016**, *8*, 22025−22031.
(14) Tripathy, A.; Sen, P.; Su, B.; Briscoe, W. H. Natural and Bioinspired Nanostructured Bactericidal Surfaces. *Adv. Colloid Interface Sci.* **2017**, *248*, 85−104.
(15) Zhou, F.; Li, D.; Wu, Z.; Song, B.; Yuan, L.; Chen, H. Enhancing Specific Binding of L929 Fibroblasts: Effects of Multi-scale Topography of GRGDY Peptide Modified Surfaces. *Macromol. Biosci.* **2012**, *12*, 1391−1400.
(16) Ma, Q. L.; Zhao, L. Z.; Liu, R. R.; Jin, B. Q.; Song, W.; Wang, Y.; Zhang, Y. S.; Chen, L. H.; Zhang, Y. M. Improved Implant Osseointegration of a Nanostructured Titanium Surface via Mediation of Macrophage Polarization. *Biomaterials* **2014**, *35*, 9853−9867.
(17) Mills, C. M1 and M2Macrophages: Oracles of Health and Disease. *Crit. Rev. Immunol.* **2012**, *32*, 463−488.
(18) Benoit, M.; Desnues, B.; Mege, J. L. Macrophage Polarization in Bacterial Infections. *J. Immunol.* **2008**, *181*, 3733−3739.
(19) Martinez, S. G. F. O. The M1 and M2 Paradigm of Macrophage Activation: Time for Reassessment. *F1000Prime Rep.* **2014**, *6*, 13−26.
(20) Sica, A.; Larghi, P.; Mancino, A.; Rubino, L.; Porta, C.; Totaro, M. G.; Rimoldi, M.; Biswas, S. K.; Allavena, P.; Mantovani, A. Macrophage Polarization in Tumour Progression. *Semin. Cancer Biol.* **2008**, *18*, 349−355.
(21) Subbiahdoss, G.; Kuijer, R.; Grijpma, D. W.; Van der Mei, H. C.; Busscher, H. J. Microbial Biofilm Growth vs. Tissue Integration: "The Race for the Surface" Experimentally Studied. *Acta Biomater.* **2009**, *5*, 1399−1404.
(22) Gristina, A. G. Biomaterial-Centered Infection: Microbial Adhesion Versus Tissue Integration. *Science* **1987**, *237*, 1588−1595.
(23) Gristina, A. G.; Naylor, P.; Myrvik, Q. Infections from Biomaterials and Implants: a Race for the Surface. *Med. Prog. Technol.* **1989**, *14*, 205−224.
(24) Moriarty, T. F.; Grainger, D. W.; Richards, R. G. Challenges in Linking Preclinical Anti-Microbial Research Strategies with Clinical Outcomes for Device-Associated Infections. *Eur. Cell Mater.* **2014**, *28*, 112−128.
(25) Knight, A. Systematic Reviews of Animal Experiments Demonstrate Poor Contributions Toward Human Healthcare. *Rev. Recent Clin. Trials* **2008**, *3*, 89−96.
(26) Subbiahdoss, G.; da Silva Domingues, J. F.; Kuijer, R.; Van der Mei, H. C.; Busscher, H. J. Bridging the Gap Between In Vitro and In Vivo Evaluation of Biomaterial-Associated Infections: Immunological Aspects and Antimicrobial Strategies. *Biomaterials Associated Infection*; Springer New York: New York, NY, 2013; pp 107−117, DOI: 10.1007/978-1-4614-1031-7_5.
(27) Yue, C.; Kuijer, R.; Kaper, H. J.; Van der Mei, H. C.; Busscher, H. J. Simultaneous Interaction of Bacteria and Tissue Cells with Photocatalytically Activated, Anodized Titanium Surfaces. *Biomaterials* **2014**, *35*, 2580−2587.
(28) Massey, R. C.; Horsburgh, M. J.; Lina, G.; Höök, M.; Recker, M. The Evolution and Maintenance of Virulence in *Staphylococcus aureus*: A Role for Host-To-Host Transmission? *Nat. Rev. Microbiol.* **2006**, *4*, 953−958.
(29) Cheung, G. Y. C.; Rigby, K.; Wang, R.; Queck, S. Y.; Braughton, K. R.; Whitney, A. R.; Teintze, M.; DeLeo, F. R.; Otto, M. *Staphylococcus epidermidis* Strategies to Avoid Killing by Human Neutrophils. *PLoS Pathog.* **2010**, *6*, e1001133.
(30) Zhao, B.; Van der Mei, H. C.; Subbiahdoss, G.; De Vries, J.; Rustema-Abbing, M.; Kuijer, R.; Busscher, H. J.; Ren, Y. Soft Tissue Integration Versus Early Biofilm Formation on Different Dental Implant Materials. *Dent. Mater.* **2014**, *30*, 716−727.
(31) Charalampakis, G.; Leonhardt, Å.; Rabe, P.; Dahlén, G. Clinical and Microbiological Characteristics of Peri-implantitis Cases: A Retrospective Multicentre Study. *Clin. Oral Implants Res.* **2012**, *23*, 1045−1054.
(32) Subbiahdoss, G.; Fernandez, I. C. S.; da Silva Domingues, J. F.; Kuijer, R.; Van der Mei, H. C.; Busscher, H. J. *In vitro* Interactions between Bacteria, Osteoblast-like Cells and Macrophages in the Pathogenesis of Biomaterial-Associated Infections. *PLoS One* **2011**, *6*, e24827.
(33) Clatworthy, A. E.; Pierson, E.; Hung, D. T. Targeting Virulence: A New Paradigm for Antimicrobial Therapy. *Nat. Chem. Biol.* **2007**, *3*, 541−548.
(34) Zhou, F.; Yuan, L.; Wang, H.; Li, D.; Chen, H. Gold Nanoparticle Layer: A Promising Platform for Ultra-Sensitive Cancer Detection. *Langmuir* **2011**, *27*, 2155−2158.
(35) Lyu, Z.; Wang, H.; Wang, Y.; Ding, K.; Liu, H.; Yuan, L.; Shi, X.; Wang, M.; Wang, Y.; Chen, H. Maintaining the Pluripotency of Mouse Embryonic Stem Cells on Gold Nanoparticle Layers with Nanoscale but not Microscale Surface Roughness. *Nanoscale* **2014**, *6*, 6959−6969.
(36) Zhong, J.; Zhang, H.; Yan, J.; Gong, X. Effect of Nanofiber Orientation of Electrospun Nanofibrous Scaffolds on Cell Growth and Elastin Expression of Muscle Cells. *Colloids Surf., B* **2015**, *136*, 772−778.
(37) Fitzgerald, R. H. Microbiologic Environment of the Conventional Operating Room. *Arch. Surg.* **1979**, *114*, 772−775.
(38) Bujisic, B.; Martinon, F. IRE1 Gives Weight to Obesity-Associated Inflammation. *Nat. Immunol.* **2017**, *18*, 479−480.
(39) Mills, C. D.; Ley, K. M1 and M2Macrophages: the Chicken and the Egg of Immunity. *J. Innate Immun.* **2014**, *6*, 716−726.
(40) Vasse, G. F.; Kühn, P. T.; Zhou, Q.; Bhusari, S. A.; Reker-Smit, C.; Melgert, B. N.; Van Rijn, P. Collagen Morphology Influences Macrophage Shape and Marker Expression *In Vitro*. *J. Immunol. Regener. Med.* **2018**, *1*, 13−20.
(41) Raes, G.; Van den Bergh, R.; De Baetselier, P.; Ghassabeh, G. H.; Scotton, C.; Locati, M.; Mantovani, A.; Sozzani, S. Arginase-1 and Ym1 Are Markers for Murine, but not Human, Alternatively Activated Myeloid Cells. *J. Immunol.* **2005**, *174*, 6561−6562.
(42) Christoffersen, T. E.; Olsen Hult, L. T.; Kuczkowska, K.; Moe, K. M.; Skeie, S.; Lea, T.; Kleiveland, C. R. *In Vitro* Comparison of the Effects of Probiotic, Commensal and Pathogenic Strains on Macrophage Polarization. *Probiotics Antimicrob. Proteins* **2014**, *6*, 1−10.
(43) Busscher, H. J.; Van der Mei, H. C.; Subbiahdoss, G.; Jutte, P. C.; Van den Dungen, J. J. A. M.; Zaat, S. A. J.; Schultz, M. J.; Grainger, D. W. Biomaterial-Associated Infection Locating the Finish. *Sci. Transl. Med.* **2012**, *4*, 153rv10.
(44) Roszer, T. Understanding the Mysterious M2Macrophage through Activation Markers and Effector Mechanisms. *Mediators Inflammation* **2015**, *2015*, 816460.
(45) Benoit, M.; Desnues, B.; Mege, J. L. Macrophage Polarization in Bacterial Infections. *J. Immunol.* **2008**, *181*, 3733−3739.
(46) Young, M. R. I.; Young, M. E.; Wright, M. A. Myelopoiesis-associated Suppressor-cell Activity in Mice with Lewis Lung Carcinoma Tumors: Interferon-γ Plus Tumor Necrosis Factor-α Synergistically Reduce Suppressor Cell Activity. *Int. J. Cancer* **1990**, *46*, 245−250.
(47) Miao, X.; Wang, D.; Xu, L.; Wang, J.; Zeng, D.; Lin, S.; Jiang, X. The Response of Human Osteoblasts, Epithelial Cells, Fibroblasts, Macrophages and Oral Bacteria to Nanostructured Titanium Surfaces: A Systematic Study. *Int. J. Nanomed.* **2017**, *12*, 1415−1430.
(48) Hotchkiss, K. M.; Reddy, G. B.; Hyzy, S. L.; Schwartz, Z.; Boyan, B. D.; Olivares-Navarrete, R. Titanium Surface Characteristics, Including Topography and Wettability, Alter Macrophage Activation. *Acta Biomater.* **2016**, *31*, 425−434.
(49) Shayan, M.; Padmanabhan, J.; Morris, A. H.; Cheung, B.; Smith, R.; Schroers, J.; Kyriakides, T. R. Nanopatterned Bulk Metallic Glass-Based Biomaterials Modulate Macrophage Polarization. *Acta Biomater.* **2018**, *75*, 427−438.
(50) Zhang, J.; Zhang, N.; Wei, W.; Guo, Q.; Wang, W.; Wang, P.; Wang, X. MicroRNA-24 Modulates *Staphylococcus aureus*-Induced

Macrophage Polarization by Suppressing CHI3L1. *Inflammation* **2017**, *40*, 995−1005.
(51) Peng, K. T.; Hsieh, C. C.; Huang, T. Y.; Chen, P. C.; Shih, H. N.; Lee, M. S.; Chang, P. J. *Staphylococcus aureus* Biofilm Elicits the Expansion, Activation and Polarization of Myeloid-Derived Suppressor Cells *In Vivo* and *In Vitro*. *PLoS One* **2017**, *12*, e0183271.
(52) Gries, C. M.; Kielian, T. Staphylococcal Biofilms and Immune Polarization During Prosthetic Joint Infection. *J. Am. Acad. Orthop. Surg.* **2017**, *25*, S20−S24.
(53) Thurlow, L. R.; Hanke, M. L.; Fritz, T.; Angle, A.; Aldrich, A.; Williams, S. H.; Engebretsen, I. L.; Bayles, K. W.; Horswill, A. R.; Kielian, T. *Staphylococcus aureus* Biofilms Prevent Macrophage Phagocytosis and Attenuate Inflammation *In Vivo*. *J. Immunol.* **2011**, *186*, 6585−6596.
(54) Gittens, R. A.; Olivares-Navarrete, R.; Schwartz, Z.; Boyan, B. D. Implant Osseointegration and the Role of Microroughness and Nanostructures: Lessons for Spine Implants. *Acta Biomater.* **2014**, *10*, 3363−3371.
(55) Hizal, F.; Rungraeng, N.; Lee, J.; Jun, S.; Busscher, H. J.; Van der Mei, H. C.; Choi, C. H. Nanoengineered Superhydrophobic Surfaces of Aluminum with Extremely Low Bacterial Adhesivity. *ACS Appl. Mater. Interfaces* **2017**, *9*, 12118−12129.
(56) Lim, J. Y.; Donahue, H. J. Cell Sensing and Response to Micro- and Nanostructured Surfaces Produced by Chemical and Topographic Patterning. *Tissue Eng.* **2007**, *13*, 1879−1891.
(57) Jeon, H.; Simon, C. G., Jr; Kim, G. A Mini-review: Cell Response to Microscale, Nanoscale, and Hierarchical Patterning of Surface Structure. *J. Biomed. Mater. Res., Part B* **2014**, *102*, 1580−1594.
(58) Schakenraad, J. M.; Busscher, H. J.; Wildevuur, C. R.; Arends, J. The Influence of Substratum Surface Free Energy on Growth and Spreading of Human Fibroblasts in the Presence and Absence of Serum Proteins. *J. Biomed. Mater. Res.* **1986**, *20*, 773−784.
(59) Arima, Y.; Iwata, H. Effect of Wettability and Surface Functional Groups on Protein Adsorption and Cell Adhesion Using Well-Defined Mixed Self-Assembled Monolayers. *Biomaterials* **2007**, *28*, 3074−3082.
(60) Ranella, A.; Barberoglou, M.; Bakogianni, S.; Fotakis, C.; Stratakis, E. Tuning Cell Adhesion by Controlling the Roughness and Wettability of 3D Micro/Nano Silicon Structures. *Acta Biomater.* **2010**, *6*, 2711−2720.

https://dx.doi.org/10.1021/acsbiomaterials.9b01518
ACS Biomater. Sci. Eng. 2020, 6, 933−945